Observational study and High Resolution Numerical Experiment for Localized Heavy Precipitation Events in Seoul metropolitan area

Joon-Woo ROH, Jung-Hoon LEE, and Jeong-Gyun PARK
Meteorological Observation Laboratory, WISE (Weather Information Service Engine)
Hankuk University of Foreign Studies / Korea Meteorological Administration
neolegacy@gmail.com

Localized heavy rainfall in Seoul in warm-season

The frequency of localized heavy rainfalls (≥ 30mm/h) in Seoul in warm-season have increased threefold in recent 30 years.

Especially, the frequency and the intensity of localized heavy precipitations have also increased in the 2000s.

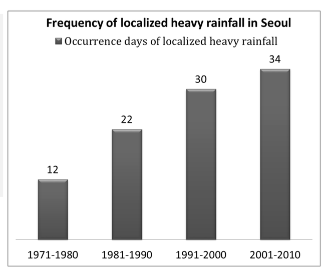

Localized heavy precipitation has occurred in very narrowed zone occasionally or simultaneously, and its period of life cycle of precipitations is very short.

Although our understanding of mechanisms for convective scale sudden and intensive precipitation in metropolitan area are still insufficient, a dominant part of mechanism for the localized concentrated precipitation is known to be due to urban artificial heat sources and construction of high-rise buildings. These have effect on the change of low level air currents over metropolitan area.

Brief review of warm-season heavy precipitation in the Korean Peninsula

Korean warm-season precipitation comprising about three-forth of the annual precipitation is mainly caused by Changma, which is a kind of the East Asian summer monsoon (Ding, 2004; Wang and Ho, 2002; Tao and Chen, 1987), convective instability between continental lows over northern China and the subtropical high over the western North Pacific, and rainfalls by the direct/indirect effect of typhoon (Lee et al., 2008; Lee, 2004; Hong, 2002).

The synoptic-scale structure related to the fronts, which are caused by a quasi-stationary moisture convergence zone or band between the tropical maritime air mass from south and continental and maritime polar air masses from north (Lee, 2005; Qian and Lee, 2000; Lau et al.,1988; Ninomiya and Mizuno, 1987; Lim et al., 2002; Wang et al., 2007; Chen et el., 2003; Ding, 2004).

There are multiple potential causes of warm-season heavy precipitation in South Korea.

Synoptic conditions producing heavy summer precipitations over Korea are characterized by strong baroclinicity. Further, it is associated with thermodynamically neutral atmosphere over Korea in contrast to large convective available potential energy, which is typical over the central US (Hong, 2004) .

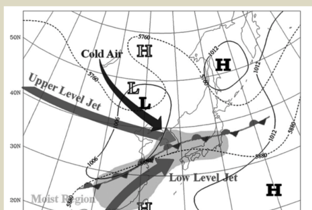

The 18-day time-mean synoptic schematic fields. SLP (solid lines), 500 hPa geopotential height (dashed lines), a high mixing ratio area (Shaded), and stationary front (Changma front) (Lee et al., 2008).

Advanced Storm-scale Analysis and Prediction System (ASAPS)

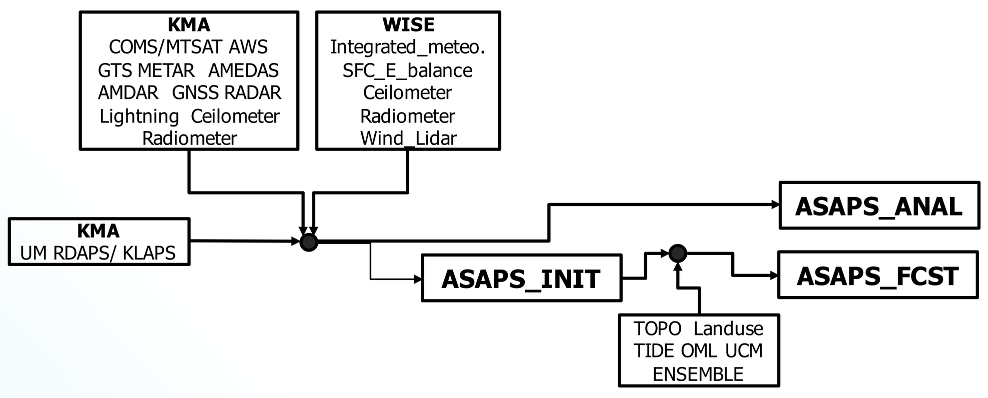

ASAPS was developed in National Institute of Meteorological Sciences (NIMS; 2013)

Improvement of initialization through analyzing observation data using Local Analysis and Prediction System (LAPS)

Forecasting based on Weather Research and Forecast (WRF)

1km horizontal resolution, rapid update with every 1 hour (30min.)

Convective scale diagnostic variable

Storm Relative Helicity (SRH)

(e.g., Davies-Jones 1990)

$$SRH = -\int_0^h \left[(\vec{V}-\vec{c})\cdot\vec{k}\times\left(\frac{\partial\vec{V}}{\partial z}\right)\right]dz$$

$$= -\int_0^h \left[-(u-c_x)\left(\frac{\partial v}{\partial z}\right)+(v-c_y)\left(\frac{\partial u}{\partial z}\right)\right]dz$$

SRH is defined as the component of the 3-dimensional vorticity vector in the direction of the storm relative flow. SRH is a measure of the potential for cyclonic updraft rotation in right-moving supercells.

Larger values of 0-3-km SRH (greater than 250 m^2/s^2) and 0-1-km SRH (greater than 100 m^2/s^2) do suggest an increased threat of tornadoes with supercells.

Large value of helicity is favorable for the formation of many kinds of extreme weather phenomena of synoptic scale to meso-β scale such as heavy precipitation and thunderstorm (Jincai et al. 1996).

SRH was applied as a parameter for heavy precipitations and gust wind in Shanghai area (Jincai et al. 1996).

Instantaneous Contraction Rate (ICON)

(e.g., Cohen, R. A., and D. M. Schultz, 2005)

$$ICON = 1/2(E - D) \qquad E = \sqrt{(E_{st}^2 + E_{sh}^2)} \quad \text{Resultant deformation}$$

$$E_{st} = \frac{\partial u}{\partial x} - \frac{\partial v}{\partial y} \quad \text{Stretching deformation}$$

$$E_{sh} = \frac{\partial u}{\partial y} + \frac{\partial v}{\partial x} \quad \text{Shearing deformation}$$

$$D = \frac{\partial u}{\partial x} + \frac{\partial v}{\partial y} \quad \text{Divergence}$$

ICON is a measure of the instantaneous rate of change of the distance between two adjacent air parcels. It is related to the process of frontogenesis, which involves an increase of the gradient in some property of the air, such as temperature or moisture, as contraction proceeds.

Horizontal vector gradient tensor magnitude (HVGTM)

(e.g. Stonitsch and Markowski, 2007)

$$|\nabla_h \overline{v_h}| = HVGTM^2 \propto DIV^2 + VOR^2 + E^2$$

The kinematic properties of the airflow are those associated with the first order partial derivatives of the horizontal velocity.

The magnitude of the tensor formed from these four partial derivatives is a measure of the combined velocity gradients in the airflow.

These four derivatives can be combined to produce three scalar quantities that are independent of the coordinate system (i.e., are invariant): the divergence (DIV), the vorticity (VOR), and the resultant deformation (E).

Strong boundaries in the airflow (wind shift lines) typically are associated with large values for one or more kinematic properties, so this parameter is useful for identifying and tracking significant airflow boundaries.

CASE1: 20140620

OBS::AWS

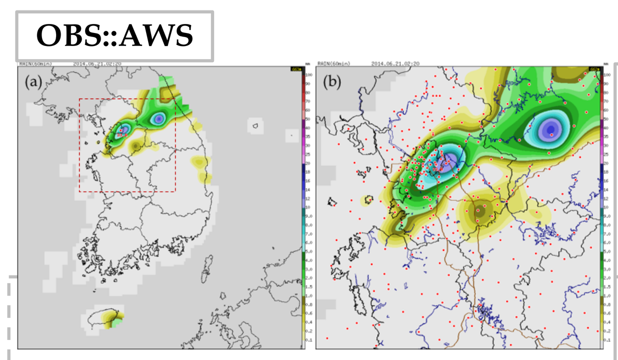

Distribution of KMA AWS observed 1-hourly accumulated precipitation amount in (a) the area of South Korea in 1720 UTC 20 June 2014. (b) shows 1-hourly accumulated precipitation amount in the area within red-dashed lines of (a).

OBS::AWS

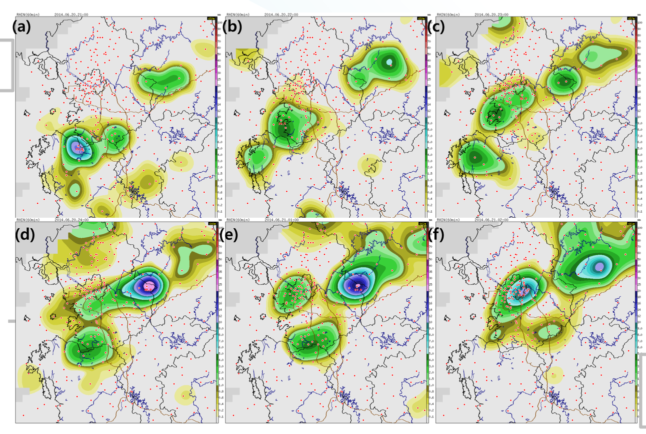

AWS:: 1200 to 1700 UTC

OBS::RADAR

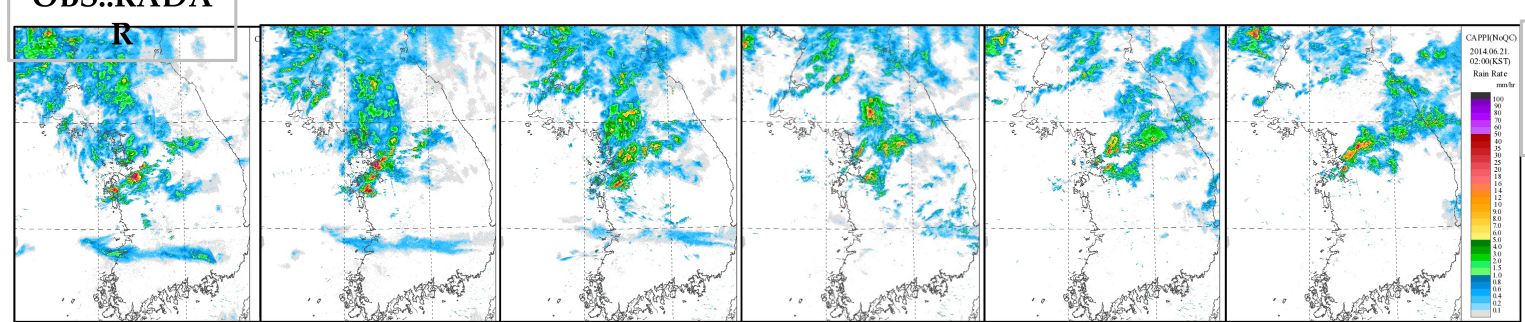

The composite of KMA radar images in 1200 UTC (e.g., 2100 KST) to 1700 UTC 20 June 2014.

OBS::Satellite

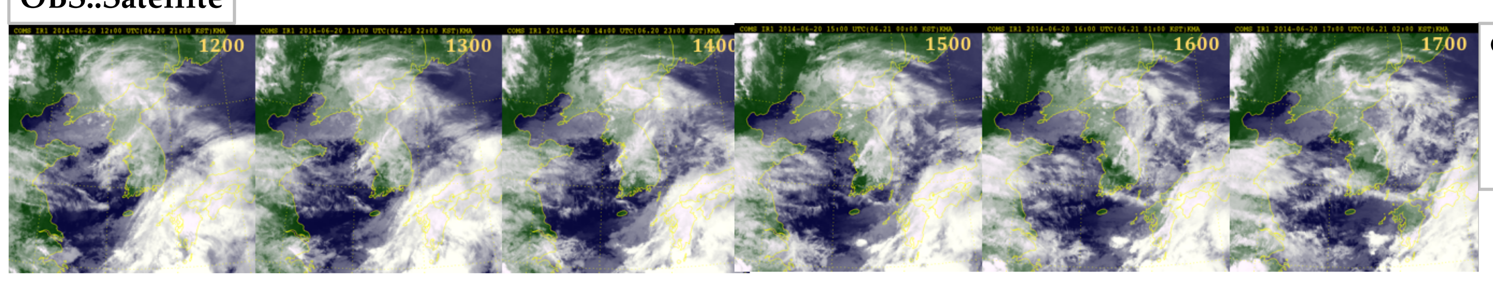

COMS Satellite infrared images from 1200 UTC to 1700 UTC 20 June 2014

ReAnalysis::FNL

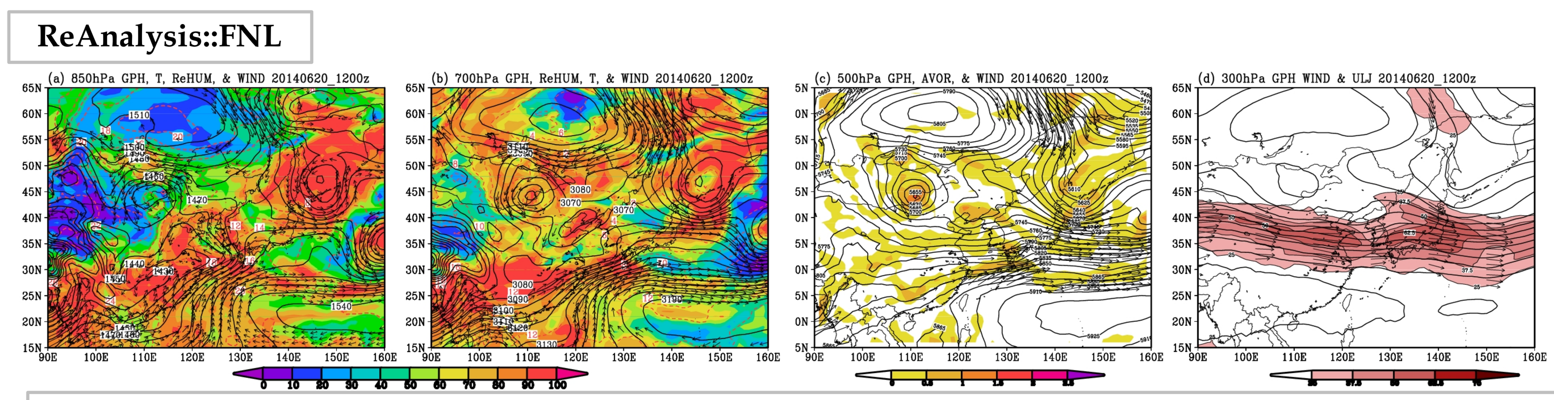

Weather charts at 1200 UTC 20 June, 2014 : (a) 850hPa GPH (contoured at 10 gpm interval with solid line), temperature (contoured at 2 ℃ interval with red dashed line), relative humidity (shaded rainbow color), and wind > 5m/sec (vector), (b) 700 hPa GPH (contoured at 10 gpm interval with solid line), temperature (contoured at 2 ℃ interval with red dashed line), relative humidity (shaded rainbow color), and wind > 8m/sec (vector), (c) 500 hPa GPH (contoured at 15 gpm interval with solid line), absolute vorticity (color shaded over $1\times10^{-4}sec^{-1}$), and wind > 15m/sec (vector), and (d) 300 hPa GPH (contoured at 60 gpm interval with solid line), upper level jet (red shaded over 75kts), and wind > 50kts (vector).

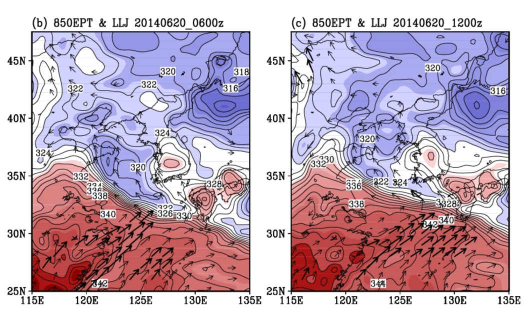

850-hPa equivalent potential temperature (blue shaded below 324K and red shaded over 330K), wind > 5m/sec (vector), & > 12.5m/sec (vector bolded)

Performance of high resolution NWP

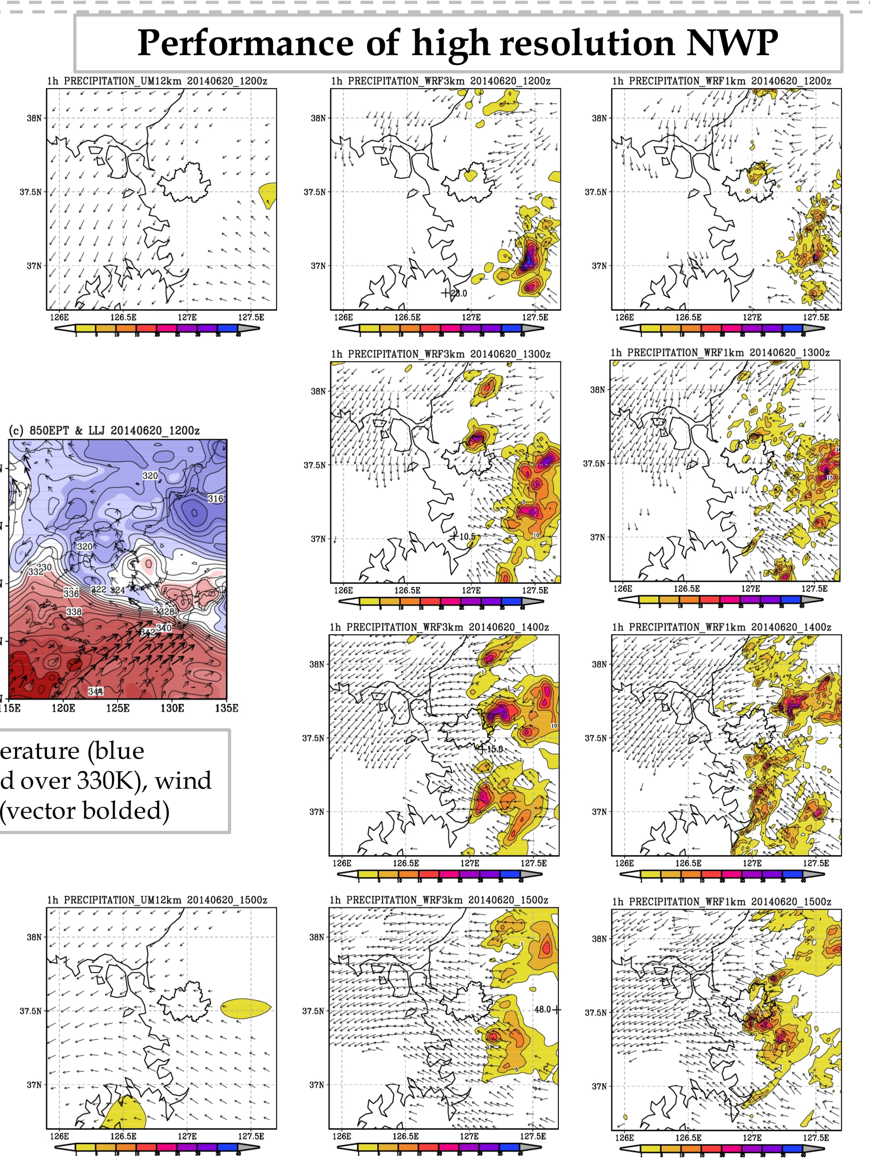

Comparison among distributions of 1-hr accumulated precipitation amounts [mm/h] and wind vector of UM12km, WRF3km, and WRF1km for EXP1 in 1200 UTC and 1500 UTC. Cross symbol and value in WRF3km panel indicates the position of the maximum 1-hr accumulated precipitation amounts [mm/h] in AWS station (see Fig.2a and Fig.2d). Wind vector (>3m/s) of UM_RDAPS at 50-m height, and wind vectors (>5m/s) of WRF3km and WRF1km at 1000-hPa height were also shown

Diagnostic variable

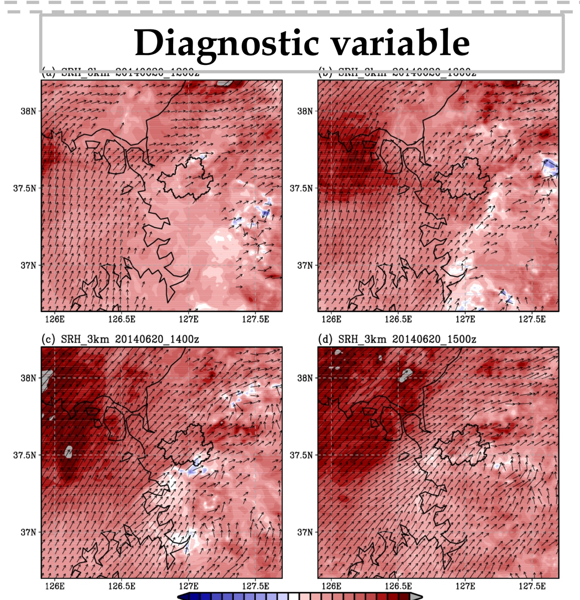

Distribution of storm relative helicity for 0-3km altitude and 700-hPa wind vector (> 4m/s) of WRF1km simulation from (a) 1200 to (d) 1500 UTC

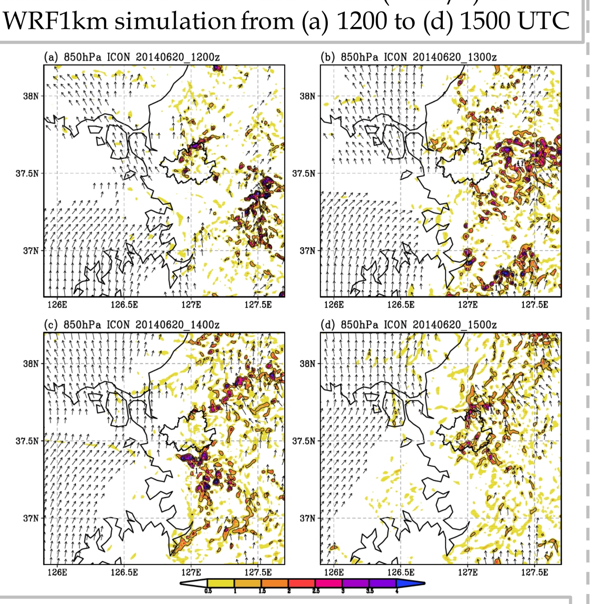

Distribution of 850-hPa instantaneous contraction rate (ICON) and 850-hPa wind vector (>4m/s)

CASE2: 201600701

OBS::AWS

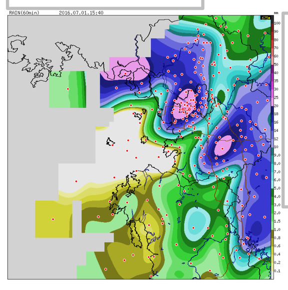

Distribution of 1-hourly accum. precipitation amount observed in KMA AWS in 0640 UTC

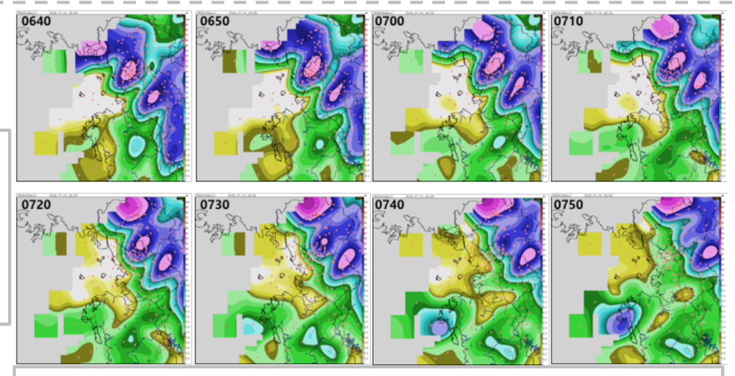

10min. interval of 1-hourly accum. precipitation amount observed in KMA AWS in 0640 UTC to 0750 UTC 1 July 2016.

OBS::Satellite

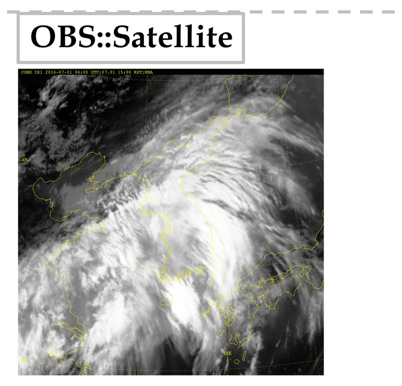

OBS::RADAR

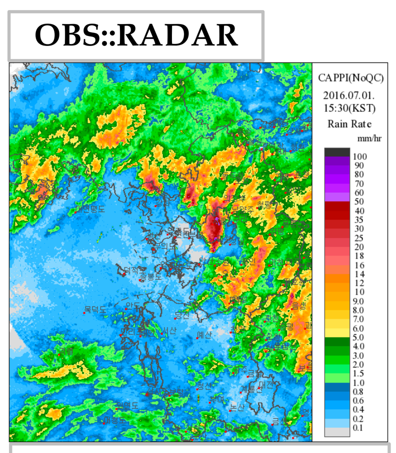

The composite of KMA radar images in 0630 UTC (1500 KST) 01 July 2016.

Storm classification technique

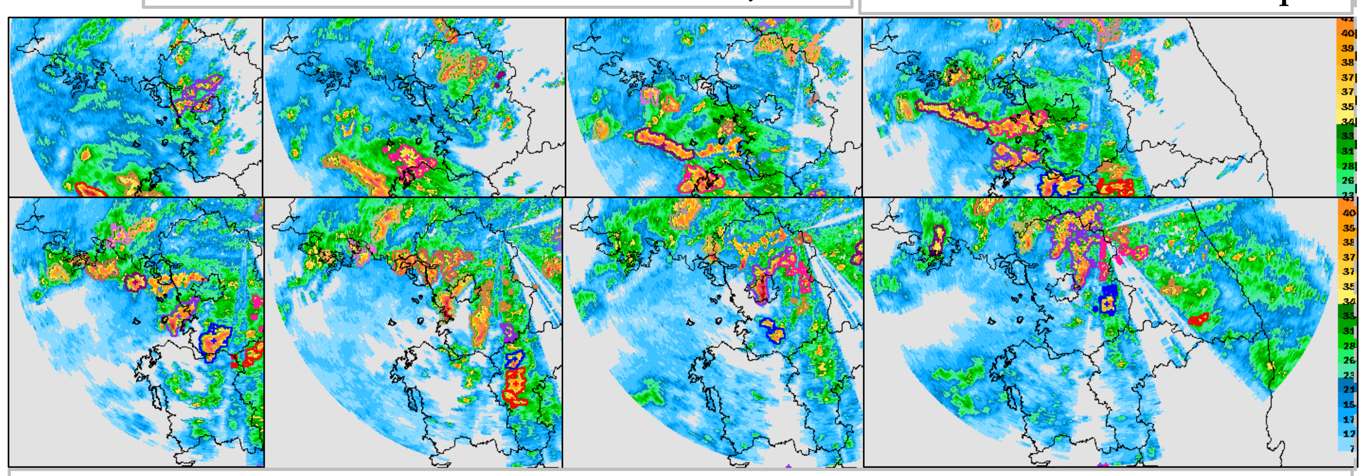

Storm classification distribution for 30 min. intv. from 0330 (1230) to 0700 UTC (1600 KST) 01 July 2016.

A localized heavy precipitation in the Korean Peninsula occurred within synoptic-scale heavy precipitation system. A storm-scale precipitation system is mainly embedded from large-scale precipitation system potentially induced by various situations.

In order to watch and analyze storm scale system with various and complex structure, a storm identification technique was adopted. Storm identification is produced by vertical components by convective-cells from CAPPI for 1km height to 9.5km height (500m intv.).

ReAnalysis::FNL

GPH (10 gpm interval with solid line)
Temperature (3 [℃] intv. / red dashed line),
Relative humidity (blue shade: 36~51% red: 80~100%)
Wind > 4m/sec (vector)

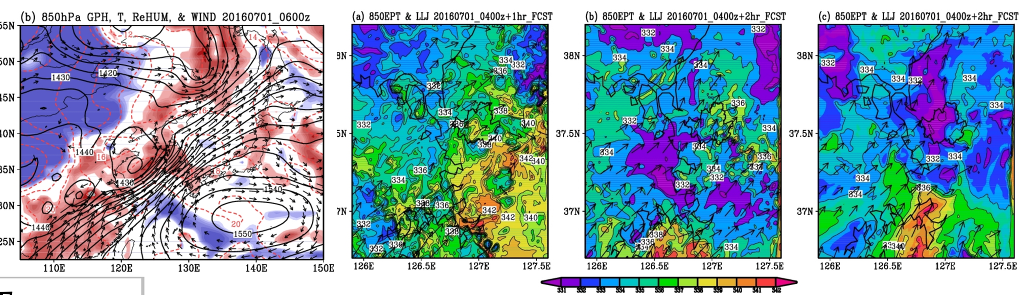

Performance of ASAPS FCST

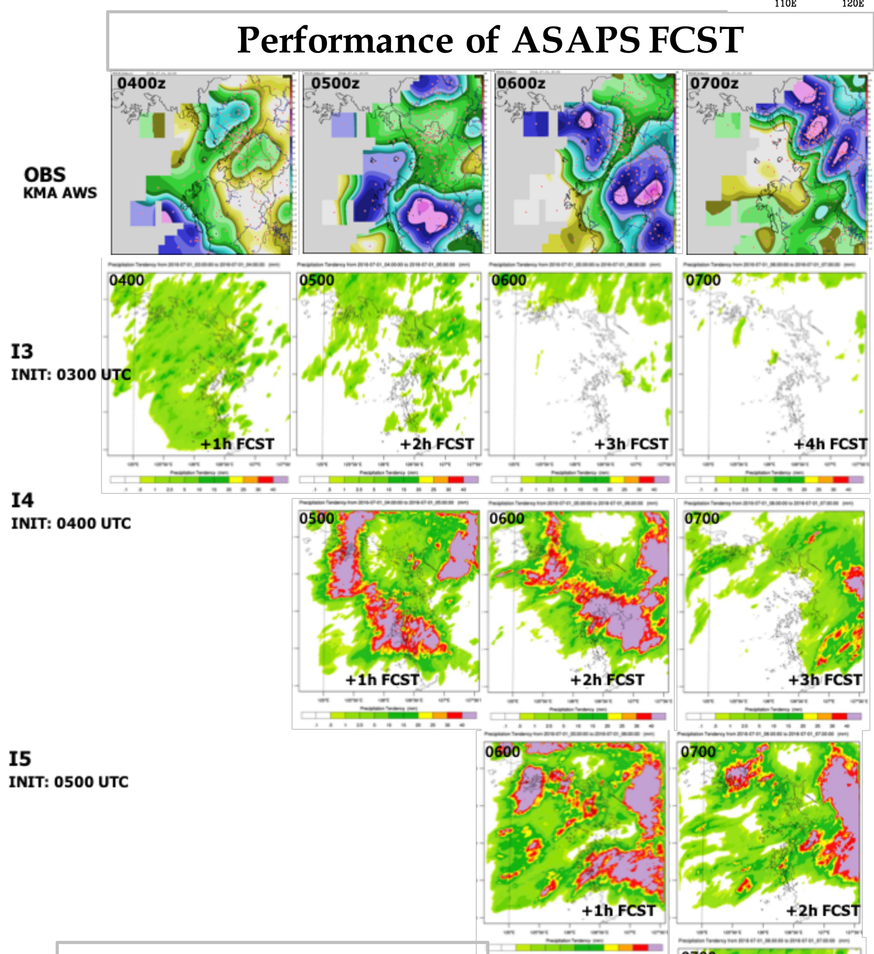

Since a localized heavy precipitation occurred in a very narrow area instantaneously, its monitoring, diagnosis and prediction are very difficult. In order to investigate a characteristic of localized heavy precipitation, observational analysis and numerical experiment for typical events.

Storm classification algorithm should be considered to describe convective precipitation and is being developed and improved for detecting convective storm and an application to convective scale quantitative precipitation Estimation. Convective scale precipitation system embedded in synoptic scale system is well observed through storm classification algorithm. Storm classification technique is very useful to detect various storm-scale heavy precipitations.

ASAPS with under 1km resolution and rapid update for targeting convective scale severe weather in the local area show a reasonable performance. The ASAPS simulations of the more recent initiation times performed better in aspect to the intensity and the location of precipitation.

In addition to, primary physical structures related to the localized heavy precipitation with the convective scale diagnostic fields, which are storm relative helicity, instantaneous contraction rates, and horizontal velocity gradient tensor magnitude, were investigated based on the ASAPS results of convective scale resolution. The physical structures of convective scale heavy precipitation system are described using diagnostic variable in more detail.

Diagnostic variable

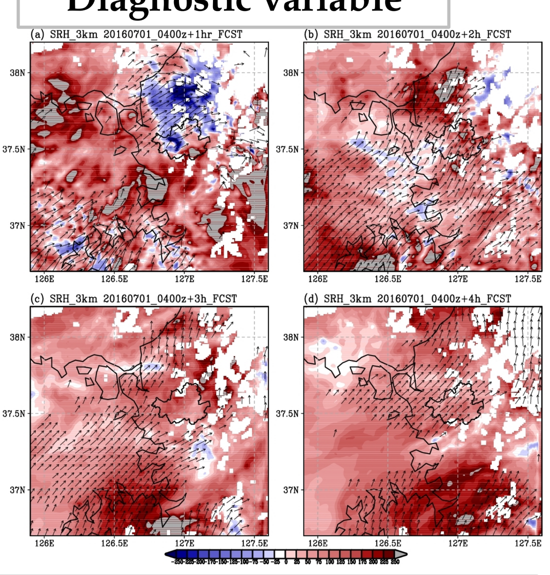

SRH for 0-3km altitude and 700-hPa wind vector (> 4m/s) from (a) 0400 to (d) 0700 UTC

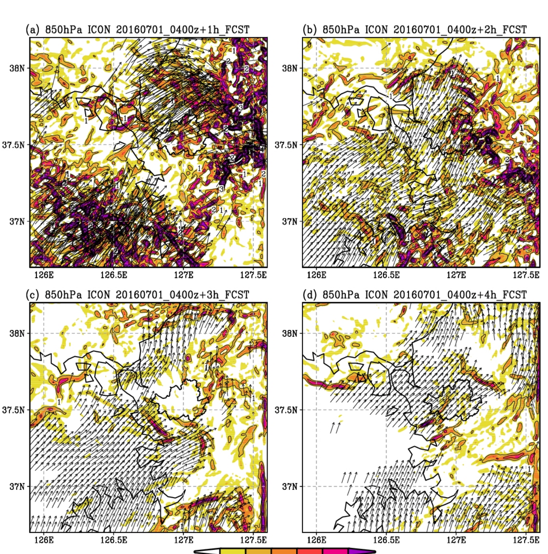

850hPa ICON and wind vector (> 4m/s) from (a) 0400 to (d) 0700 UTC

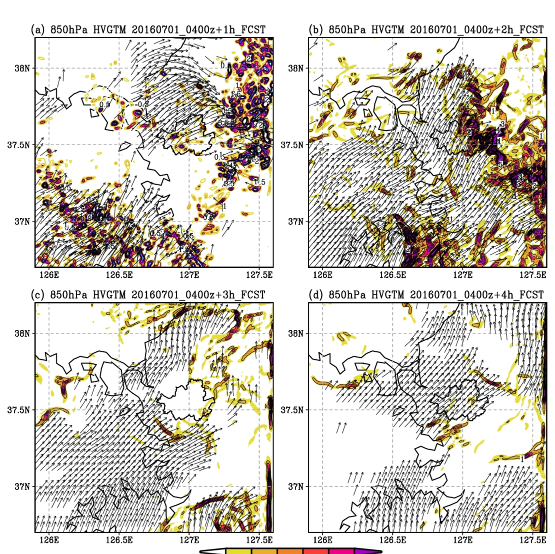

850-hPa HVGTM and wind vector (> 4m/s) from (a) 0400 to (d) 0700 UTC

Korea Meteorological Administration
HANKUK UNIVERSITY OF FOREIGN STUDIES
W'ISE Weather Information Service Engine

This work was funded by the Weather Information Service Engine Program of the Korea Meteorological Administration under Grant KMIPA-2012-0001-1